ANFIS Based Speed Controller for a Direct Torque Controlled Induction Motor Drive

Hadhiq Khan, Shoeb Hussain, Mohammad Abid Bazaz

Abstract This paper presents a Neuro-Fuzzy adaptive controller for speed control of a three phase direct torque controlled induction motor drive. The Direct Torque Control (DTC) scheme is one of the most advanced methods for controlling the flux and electromagnetic torque of machines. Control of electromagnetic torque/speed in these drives for high performance applications requires a highly robust and adaptive controller. Adaptive Neural-Fuzzy Inference System (ANFIS) is a hybrid between Artificial Neural Networks (ANN) and Fuzzy Logic Control (FLC) that enhances the execution of direct torque controlled drives and overcomes the difficulties in the physical implementation of high performance drives.

MATLAB/SIMULINK implementation of 15 hp, 50 Hz, 4 pole squirrel cage induction motor controlled with the DTC scheme is presented in this paper. The PI controller used for speed control in conventional DTC drives is substituted by the ANFIS based controller. Simulation results show the use of ANFIS decreases the response time along with reduction in torque ripples.

1 Introduction

Squirrel cage induction motors find applications in motor driven pumps, washing machines, air conditioning and heating systems, servo drives, hybrid electric vehicles, domestic appliances etc. Low price, small size and weight, rugged and robust

Hadhiq Khan
Department of Electrical Engineering, NIT Srinagar, Email: hadhiqkhan@gmail.com
Shoeb Hussain
Department of Electrical Engineering, NIT Srinagar, Email: shoeb_ 15phd13@nitsri.net
Mohammad Abid Bazaz
Department of Electrical Engineering, NIT Srinagar, Email: abid@nitsri.net

J.M. Corchado Rodriguez et al. (eds.), *Intelligent Systems Technologies and Applications 2016*, Advances in Intelligent Systems and Computing 530,
DOI 10.1007/978-3-319-47952-1_71

contruction, the absence of commutators and brushes are some of the distinct advantages that make induction motors the most preferred motors in electric drive systems.

Induction motors happen to be constant speed motors. With the use of power electronic converters, induction motors can be employed in variable speed applications. To interface between the fixed voltage and frequency utility supply with motors, power electronic converters are used. High frequency and low loss power semiconductor devices are being increasingly used for manufacturing efficient converters.

Compared to the control of dc motors, the control of induction motors is difficult owing to the fact that the induction motor is a dynamic, nonlinear system. Unpredictable disturbances such as noise and load changes and the uncertainties in the machine parameters further complicate the control problem.

To reduce the complex nonlinear structure, advanced control techniques such as field oriented control (FOC) [1], [2] and direct torque control (DTC) [3], [4] have been developed offering fast and dynamic torque response. The DTC scheme, as the name indicates is a direct control of the torque and flux of the machine. The electromagnetic torque and the flux generated in the machine is compared to the reference values of the torque and flux in hysteresis comparators. The outputs of the two comparators along with the stator flux position determine the voltage vector from a lookup table.

For controlling the various states of the inverter, control pulses are generated. The output of the inverter is eventually fed to the induction motor.

Even though FOC and DTC methods have been effective, a number of drawbacks are observed (distortions in currents and torque due to change in the flux sector, the need for high sampling frequency for digital implementation of the comparators, sensitivity to variations in the machine parameters etc).

To mitigate the shortcomings in the DTC scheme, intelligent control techniques using human motivated techniques, pattern recognition and decision making are being adopted [5], [6]. Some of the methods based on the concept of Artificial intelligence (AI) are Artificial Neural Network (ANN), Expert System (ES), Fuzzy Logic Control (FLC) to mention a few. AI based techniques when implemented in motor control have shown improved performance [7].

Generally, motor control drives rely on the use of PI controllers. These controllers, however, are sensitive to system non-linearities, variations in parameters and any unwanted disturbances. These disadvantages can be overcome by the use of AI based intelligent controllers. Fuzzy logic and artificial neural networks are two of the most popular systems for use as intelligent controllers and have shown an improved performance over conventional controllers [8], [9], [10]. ANFIS (adaptive neural network based fuzzy inference system), a hybrid of ANN and FLC is another popular control scheme being used in high performance drives, having superior design and performance characteristics [6].

The use of an ANFIS based speed controller for a direct torque controlled induction motor drive is presented in this paper. The PI controller used in the conventional DTC scheme is replaced with the ANFIS based speed controller.

The paper is arranged in the following sections: Section 2 presents the dynamic dynamic-quadrature axis model of the motor. The concept of direct torque control is introduced in Section 3 followed by the control strategy in Section 4. The ANFIS speed controller is presented in Section 5 followed by the simulation results and conclusion in Sections 6 and 7 respectively.

2 D - Q Model of Induction Motor

At the core of the induction motor DTC scheme lies the dynamic direct-quadrature axis model of the induction motor. The steady state model of the induction motor is useful only if the steady state characteristics of the motor are to be studied. For high performance drives, the transient as well as the steady state response needs to be taken into account which is not possible without the use of the d-q model. A detailed description of the model is illustrated in [11].

The generalised state equations governing the dynamics of the motor rotating with a mechanical speed ω_r are:

$$\frac{dF_{qs}}{dt} = \omega_b \left[v_{qs} - \frac{\omega_e}{\omega_b} F_{ds} - \frac{R_s}{X_{ls}} \left(F_{qs} - F_{qm} \right) \right] \tag{1}$$

$$\frac{dF_{ds}}{dt} = \omega_b \left[v_{ds} + \frac{\omega_e}{\omega_b} F_{qs} - \frac{R_s}{X_{ls}} \left(F_{ds} - F_{dm} \right) \right] \tag{2}$$

$$\frac{dF_{qr}}{dt} = -\omega_b \left[\frac{(\omega_e - \omega_r)}{\omega_b} F_{dr} + \frac{R_r}{X_{lr}} \left(F_{qr} - F_{qm} \right) \right] \tag{3}$$

$$\frac{dF_{dr}}{dt} = -\omega_b \left[\frac{-(\omega_e - \omega_r)}{\omega_b} F_{qr} + \frac{R_r}{X_{lr}} \left(F_{dr} - F_{dm} \right) \right] \tag{4}$$

$$F_{qm} = \frac{X_{ml}}{X_{ls}} F_{qs} + \frac{X_{ml}}{X_{lr}} F_{qr} \tag{5}$$

$$F_{dm} = \frac{X_{ml}}{X_{ls}} F_{ds} + \frac{X_{ml}}{X_{lr}} F_{dr} \tag{6}$$

$$X_{ml} = \frac{1}{\frac{1}{X_m} + \frac{1}{X_{ls}} + \frac{1}{X_{lr}}} \tag{7}$$

where the flux linkage state variable is denoted by F. ds and qs in subscripts correspond to the dynamic and quadrature axis stator variables. dr and qr in subscripts refer to the rotor variables. ω_b is the base frequency of the machine. ω_e is the frequency of an arbitrarily rotating reference frame. All calculations in the DTC scheme discussed in this paper are performed in the stationary reference frame, with

ω_e set to 0. The motor currents are obtained from the flux linkages as:

$$i_{qs} = \frac{F_{qs} - F_{qm}}{X_{ls}}, \quad i_{qr} = \frac{F_{qr} - F_{qm}}{X_{lr}} \tag{8}$$

$$i_{ds} = \frac{F_{ds} - F_{dm}}{X_{ls}}, \quad i_{dr} = \frac{F_{dr} - F_{dm}}{X_{lr}} \tag{9}$$

Detailed simulations of the model presented above is explained in [12].

3 Direct Torque Control

The direct torque control scheme was introduced by Depenbrock and Takahashi [3], [4] in the 1980s. The performance of the DTC scheme is comparable to that of other field oriented control methods and is simpler to implement. The need for repeated transformations from one reference frame to another, as in case of FOC drives is eliminated as all the calculations are performed in a single reference frame.

The electromagnetic torque and the stator flux developed in the machine are compared to their respective reference values which are input to hysteresis comparators. The outputs of the two hysteresis comparators along with the position of the vector of the stator flux generates control signals which are fed to a voltage source inverter (VSI). The VSI in turn, drives the induction motor mode [13].

The fundamental assumption in DTC is that if the stator resistance voltage can be taken to be equal to zero, the flux in the stator of the induction motor can be assumed to be equal to the integration of the voltage. Alternatively, the applied voltage can be thought to be equal to the time derivative of the stator flux. The relationship between the stator flux and the applied voltage can be thus expressed as:

$$\bar{V}_s = \frac{d}{dt}(\bar{\psi}_s) \tag{10}$$

or

$$\Delta\bar{\psi}_s = \bar{V}_s.\Delta t \tag{11}$$

A closer look at these equations reveals that the we can change $\bar{\psi}_s$, the stator flux, by applying an appropriate the stator voltage $\bar{V}_s$ for time Δt.

The output voltage of the inverter, therefore, is impressed upon the stator flux vector. To obtain a desired value of the flux of the stator, appropriate voltage vectors have to be applied [14]. For short transients, the rotor flux is assumed to be constant since the rotor time constant is significantly large.

Flux and torque references are the command inputs of the control scheme. When the system is operated in the torque control mode, a torque input is applied, whereas in the speed control mode, the reference speed is input to a PI controller which translates the signal to an equivalent torque reference to be input to the system. Magnitudes of the stator flux and torque are estimated from the d-q model. Comparison between the calculated and the reference values is done. Flux and torque hysteresis bands, between which the two quantities are allowed to vary, are de-

fined. If the errors fall outside the hysteresis bands, appropriate control signals to increase/decrease the torque and flux are required.

The location of the stator flux vector in space is also to be calculated. A two dimensional complex plane is divided into six sectors which span 60 degrees each. A total of eight voltage vectors V_0 through V_7 are defined. The vectors V_0 and V_7 maintain the torque and flux constant and hence are called zero vectors. Vectors V_1 through V_6 are active vectors responsible for increasing/decreasing flux and torque.

After each sampling interval, appropriate voltage vectors are selected to keep the stator flux and electromagnetic torque within limit [15]. The width of the hysteresis band has a direct influence on the inverter switching frequency. With a decrease in width of the band, the switching frequency increases. The switching frequency of the VSI is low when a wide hysteresis band is set. Consequently, the system response is poor.

4 Control Scheme

The basic dircect torque control scheme of an induction motor has two parallel modes: for controlling flux and torque respectively. The flux reference is directly input to the system in the first mode while as the reference torque (taken as the output of the speed controller) is the input in the second mode. A signal computation block is used to compute the values of the electromagnetic torque, the stator flux magnitude and the sector of the stator flux vector. Hysteresis controllers, whose input are the estimated and the reference quantities, produce digital outputs. The outputs of these controllers along with the sector location are used to generate control signals for the VSI. The inverter output voltages are in turn fed to the induction motor.

4.1 Signal Estimation Block

The stator d - axis and q - axis flux magnitudes can be estimated using the relations:

$$\psi_{ds} = \int \left(v_{ds} - R_s i_{ds}\right) dt, \quad \psi_{qs} = \int \left(v_{qs} - R_s i_{qs}\right) dt \tag{12}$$

$$|\psi_s| = \sqrt{\psi_{ds}^2 + \psi_{qs}^2} \tag{13}$$

The electromagnetic torque can be estimated using the relation :

$$T_e = \frac{3}{2}\frac{P}{2}\frac{1}{\omega_b}\left(\psi_{ds} i_{qs} - \psi_{qs} i_{ds}\right) \tag{14}$$

Six sectors, each spanning an angle $\frac{\pi}{3}$ are defined in a two dimensional complex plane. The location of the flux space vector in the complex plane can be calculated

by:

$$\phi_s = \tan^{-1}\left(\frac{\psi_{qs}}{\psi_{ds}}\right) \tag{15}$$

The value of the sector angle is used to select in the voltage vector.

4.2 Hysteresis Controllers

In this block, the estimated and reference values of torque and stator flux are compared. Appropriate commands to increasing or decreasing torque and flux are generated to keep both of them within their respective hysteresis bands. In case an increment in stator flux is required, $\Delta\psi_s = 1$ and for a decrement $\Delta\psi_s = -1$

$$\Delta\psi_s = 1 \quad if \quad |\psi_s| \leq |\psi_s^*| - |hysteresis\ band| \tag{16}$$

$$\Delta\psi_s = -1 \quad if \quad |\psi_s| \geq |\psi_s^*| + |hysteresis\ band| \tag{17}$$

To increase the electromagnetic torque $\Delta T_e = 1$, to decrease torque $\Delta T_e = -1$. To keep torque constant, $\Delta T_e = 0$. A three level control is used for controlling torque and a two level control for controlling flux [11]:

$$\Delta T_e = 1 \quad if \quad T_e \leq T_e^* - |hysteresis\ band| \tag{18}$$

$$\Delta T_e = 0 \quad if \quad T_e = T_e^* \tag{19}$$

$$\Delta T_e = -1 \quad if \quad T_e \geq T_e^* + |hysteresis\ band| \tag{20}$$

4.3 Inverter Switching Table

Table 1 shows the outputs of the hysteresis comparators with the sector number. The voltage vectors corresponding to the hysteresis outputs and the sector numbers are shown. The switch positions to obtain the desired vector are given in the following table:

Table 1: Voltage Vector Switching

Output of Hysteresis Controller		Number of the Sector					
		1	2	3	4	5	6
$\Delta\psi_s$ = +1	ΔT_e = +1	$\mathbf{V_2}$	$\mathbf{V_3}$	$\mathbf{V_4}$	$\mathbf{V_5}$	$\mathbf{V_6}$	$\mathbf{V_1}$
	ΔT_e = 0	$\mathbf{V_0}$	$\mathbf{V_7}$	$\mathbf{V_0}$	$\mathbf{V_7}$	$\mathbf{V_0}$	$\mathbf{V_7}$
	ΔT_e = -1	$\mathbf{V_6}$	$\mathbf{V_1}$	$\mathbf{V_2}$	$\mathbf{V_3}$	$\mathbf{V_4}$	$\mathbf{V_5}$
$\Delta\psi_s$ = -1	Δ_{Te} = +1	$\mathbf{V_3}$	$\mathbf{V_4}$	$\mathbf{V_5}$	$\mathbf{V_6}$	$\mathbf{V_1}$	$\mathbf{V_2}$
	ΔT_e = 0	$\mathbf{V_7}$	$\mathbf{V_0}$	$\mathbf{V_7}$	$\mathbf{V_0}$	$\mathbf{V_7}$	$\mathbf{V_0}$
	ΔT_e = -1	$\mathbf{V_5}$	$\mathbf{V_6}$	$\mathbf{V_1}$	$\mathbf{V_2}$	$\mathbf{V_3}$	$\mathbf{V_4}$

Table 2: Switch States and Voltage Vectors

	$\mathbf{V_0}$	$\mathbf{V_1}$	$\mathbf{V_2}$	$\mathbf{V_3}$	$\mathbf{V_4}$	$\mathbf{V_5}$	$\mathbf{V_6}$	$\mathbf{V_7}$
S_A	0	1	1	0	0	0	1	1
S_B	0	0	1	1	1	0	0	1
S_C	0	0	0	0	1	1	1	1

The DTC scheme uses a VSI to drive the induction motor model. The primary function of the inverter is the conversion of control signals to voltage signals which are fed to the motor. Signals $S_{A,B,C}$ control the states of the inverter. For the three phases, a total of six switches are used. For each phase, two swiches are provided. When signal S_A is 1, the switch A_h is swicthed on and A_l is switched off. Similarly, when the signal S_A is 0, A_h is switched off and A_l is switched on. The same procedure fashion, the other switches can be controlled. The voltage vector which is the output of the VSI is [16] :

$$\mathbf{V}_s = \frac{2}{3} V_{dc} \left(S_A + e^{j\frac{2\pi}{3}} S_B + e^{j\frac{4\pi}{3}} S_C \right) \tag{21}$$

5 ANFIS Speed Controller

An induction motor drive controlled by the DTC has two modes of operation: The *Torque Control* mode in which the input to the system is a reference torque. The second mode is the *Speed Control* mode where a PI controller is used whose input is the difference between the reference speed and the actual speed of the motor [17].

In high performance drives, a number of control strategies are available for use as speed controllers. Fuzzy logic, neural networks and other intelligent control techniques are increasingly being implemented in control applications demanding high precision.

ANFIS is a hybrid scheme which combines fuzzy logic and artificial neural network [18]. The principles of fuzzy logic and neural networks are combined to create a better system with and enhanced design and superior performance.

In an ANFIS, a neural network is used to design a fuzzy inference system. If the input/output mappings are available for a fuzzy system, the neural network training method can be used to design the membership functions and the rule table of the fuzzy model.

The ANN is based on the concept of input/output mapping. It is trained to associate patterns between the inputs and the output analogous to how the brain works. Given a set of input data, the network is trained to produce a corresponding output pattern.

Proper mapping between the input and output can be made possible by appropriately adjusting the weights, which relate the input and the output. The training is initiated with random weights.A comparison between the output pattern for a given input with the desired output pattern is made. The weights are accordingly adjusted with each iteration till the error between the computed and the desired values falls within acceptable limits. At the termination of the training process, the network must

be in a position to recall all the input and output patterns and if required, should be able to perform interpolation and extrapolation by little amounts.

A fuzzy inference system maps input characteristics to input membership functions, input membership functions to rules. The rules are mapped to a set of output characteristics which in turn are mapped to output characteristics. The output characteristics are mapped to output membership functions which ultimately terminated as output membership functions, and the output membership functions to the output. Two of the most popular fuzzy inference systems are the Mamdani [19] and the Sugeno [20] systems.

In this paper, the speed controller is based on ANFIS. Depending on a certain training scenario, the ANFIS controller is provided with a data set. It comprises complete information of the process under various operating conditions. A proper value of torque is provided based on the measured and the reference speed [21]. Both the input as well as the target data are contained in the data set. The ANFIS controller trains the fuzzy system on the based on this data set. To train the fuzzy inference system, a neural network is used [8].

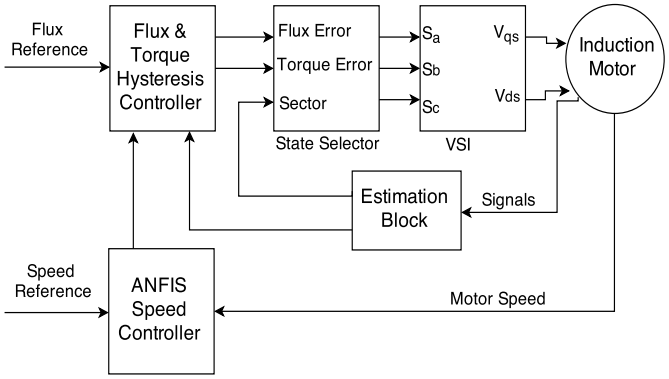

Fig. 1: ANFIS Based DTC Scheme

Figure 2 shows the ANFIS structure. It consists of five layers. The input layer contains the information about the reference and measured speeds and the error between the two. The input membership functions of the fuzzy system occupies the second layer of the system. A 7*7 gaussian membership function type system is selected. The third layer is used to generate the rules of the fuzzy system. The fourth layer is the output membership function layer. The output membership functions are constant values in a Sugeno based fuzzy system. Finally, in the output layer, the activated control signal is generated by processing the weighted signal through an activation function [18].

The back-propagation algorithm is used to compare the output pattern of the neural network with the desired output pattern. Supervised learning technique is used to train the controller. The control signal is fed forwards and the error is fed backwards. A reduction in error is possible if the number of iterations is increased. The fuzzy system is to be trained. This is done by adjusting the weights to reduce the error. After adjusting the final weights, rules governing the fuzzy system, the input membership function and the output membership function are obtained. Figure 3 shows the input membership functions. The ANFIS thus derived is used for controlling the speed of the induction motor drive.

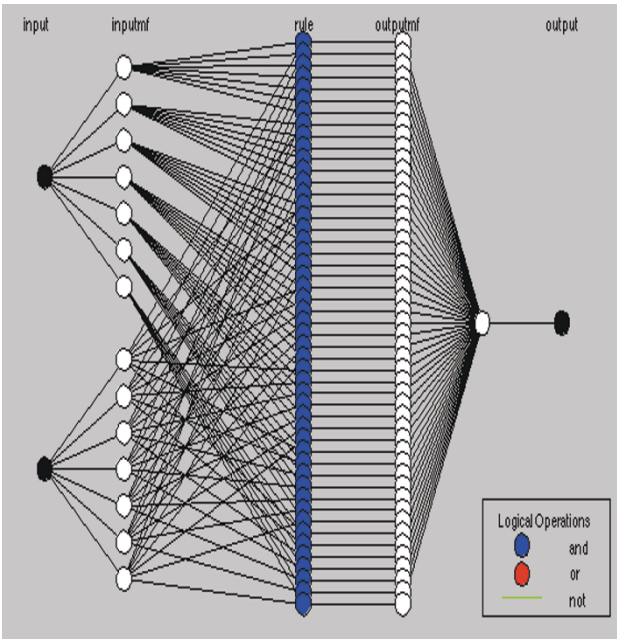

Fig. 2: ANFIS Structure

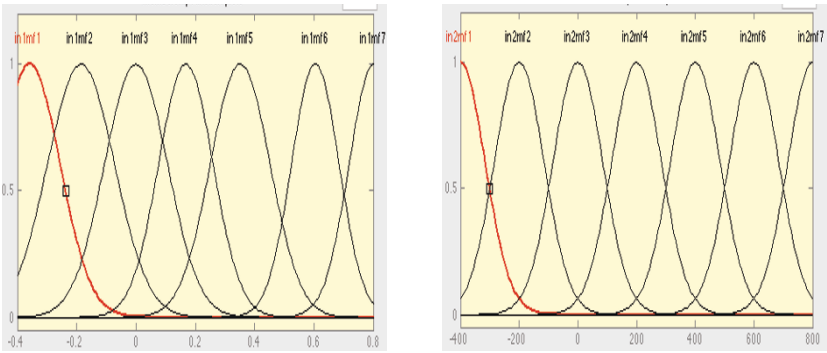

(a) Input 1 (b) Input 2

Fig. 3: Membership Functions

6 Simulation Results

To analyze the performance of the DTC induction motor drive a SIMULINK model was created. The PI controller of the conventional DTC drive was replaced by an ANFIS. A 15hp, 400V, 50Hz squirrel cage induction motor was used to study the dynamics of the drive. The induction motor parameters are given in Table 3.

The motor is initially set to run at a speed of −200 rad/s; A step input of 250 rad/s is applied at time t = 0.12 seconds. The dynamic behaviour of the motor is illustrated in the following figures. The ANFIS controller has the ability to follow the speed of the induction motor drive effectively. No considerable offset is observed. The motor reaches the set speed of −200 rad/s in 0.05 seconds. The ANFIS controller shows a faster response in comparison to the PI speed controller.

The variations of electromagnetic torque in the two schemes are shown in figures 7 and 8. The conventional PI speed controller based scheme shows considerable ripple in the torque. With the use of ANFIS, the ripple is reduced. The torque settles at the steady state value of 10 Nm which is the load torque.

Table 3: Motor Parameters

Output Power(hp)	15
Resistance (Stator) R_s, Ω	0.371
Resistance (Rotor) R_r, Ω	0.415
Leakage Inductance (Stator) L_{ls}, mH	2.72
Leakage Inductance (Rotor) L_{lr}, mH	3.3
Inductance (Magnetizing) L_m, mH	84.33
Frequency (base) ω_b, rad/s	314
Inertia J, kgm^2	0.02
DC Voltage V_{dc}, V	400
Poles P	4

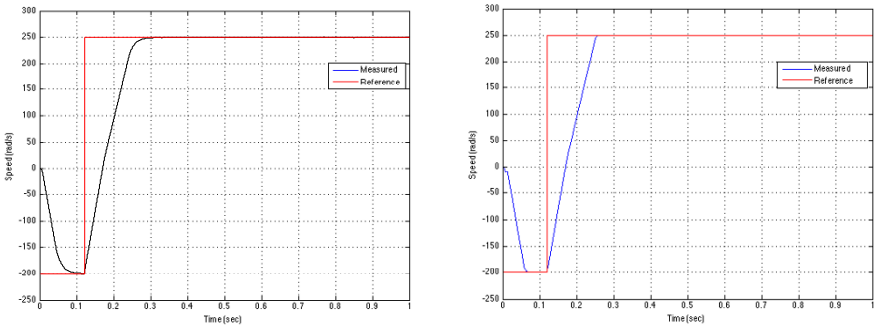

(a) Conventional Control (b) ANFIS Based Control

Fig. 4: Mechanical Speed v/s Time

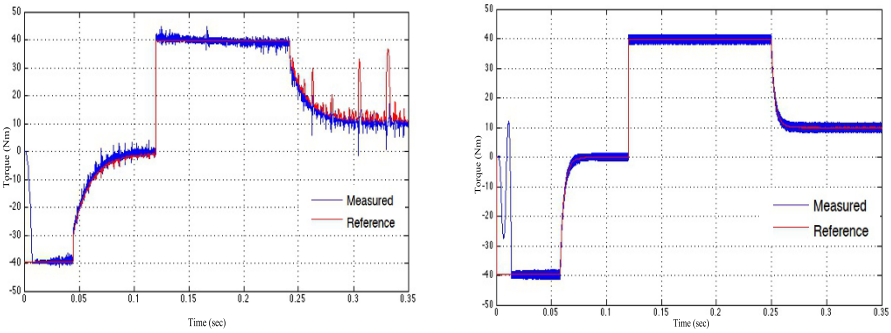

(a) Conventional Control (b) ANFIS Based Control

Fig. 5: Electromagnetic Torque v/s Time

7 Conclusion

ANFIS implementation for an induction motor drive has been presented in this paper. Different operating conditions have been studied through simulations.

When compared with conventional controllers, it is seen that with the use of ANFIS for speed control, the speed of the drive can be regulated more efficiently. Forward and reverse motoring mode speeds have been tracked and the drive system shows a smooth transition between the two modes. The ripple in the electromagnetic torque is considerably reduced. Also, the response time of the system is reduced.

References

1. F. Blaschke (1972) The Principle of Field Orientation as Applied to The New Transvector Closed Loop Control System for Rotating Field Machines. Siemens Review
2. K. Hasse (1968) On The Dynamic Behavior of Induction Machines Driven by Variable Frequency and Voltage Sources. ETZ Archive.
3. M. Depenbrock (1988) Direct Self Control (DSC) of inverter-fed induction machines. IEEE Transactions on Power Electronics
4. I. Takahashi and T. Nogushi (1986) A New Quick Response and High Efficiency Control Strategy of an Induction Motor. IEEE Transactions on Industry Applications
5. K. S. Narendra and S. Mukhopadhyay (1996) Intelligent Control Using Neural Networks. IEEE Press, New York.
6. Bimal K. Bose (1997) Expert System, Fuzzy Logic and Neural Networks in Power Electronics and Drives. IEEE Press, New Jersey
7. Tze-Fun Chan and Keli Shi (2011) Applied Intelligent Control of Induction Motor Drives. John Wiley and Sons.
8. Shoeb Hussain and Mohammad Abid Bazaz (2014) ANFIS Implementation on a Three Phase Vector Controlled Induction Motor with Efficiency Optimisation. In : International Conference on Ciruits, Systems, Communication and Information Technology (CSCITA)
9. M. Godoy Simces and Bimal K. Bose (1995) Neural Network Based Estimation of Feedback Signals for a Vector Controlled Induction Motor Drive. IEEE Transactions on Industry Applications
10. M. Nasir Uddin, Tawfik S. Radwan, and M. Azizur Rahman (2002) Performances of Fuzzy-Logic-Based Indirect Vector Control for Induction Motor Drive. IEEE Trans. Industry Applications
11. Bimal K. Bose (2002) Modern Power Electronics and AC Drives. Pearson Education Inc.
12. Adel Aktaib, Daw Ghanim and M. A. Rahman (2011) Dynamic Simulation of a Three-Phase Induction Motor Using MATLAB Simulink. In 20th Annual Newfoundland Electrical and Computer Eng. Conference (NECEC).
13. J.R.G. Schofield (1995) Direct Torque Control - DTC of Induction Motors. In IEEE Colloquium on Vector Control and Direct Torque Control of Induction Motors.
14. Peter Vas (1998) Sensorless Vector and Direct Torque Control. Oxford University Press.
15. A. Kumar, B.G. Fernandes, and K. Chatterjee (2004) Simplified SVPWM - DTC of 3 phase Induction Motor Using The Concept of Imaginary Switching Times. In: The 30th Annual Conference of the IEEE Industrial Electronics Society, Korea.
16. H.F. Abdul Wahab and H. Sanusi (2008) Simulink Model of Direct Torque Control of Induction Machine. American Journal of Applied Sciences
17. Haitham Abu-Rub, Atif Iqbal and Jaroslaw Guzinski (2012) High Performance Control of AC Drives. John Wiley and Sons.
18. J.S.R. Jang (1993) ANFIS: Adaptive-Network-Based Fuzzy Inference System. IEEE Transactions on Systems, Man and Cybernetics
19. E. H. Mamdani and S. Assilian (1975) An Experiment in Linguistic Synthesis with a Fuzzy Logic Controller. International Journal of Man-Machine Studies
20. M. Sugeno (1985) Industrial Applications of Fuzzy Control. Elsevier Science Pub. Co.
21. C. T. Lin and C. S. George Lee (1996) Neural Fuzzy Systems: A Neuro-Fuzzy Synergism to Intelligent Systems. Prentice Hall.